

**APPENDIX I.**  
**CONFIRMATORY ANALYSIS: EFFECT OF THE SUMP INTERSTITIAL VOLUME**  
**BLOCKAGE ON THE HEAD LOSS EXPERIENCED**

I. Major Relationships

Assuming that the blocked screen area is proportional to the ratio of the volume of fibrous debris blocking the sump interstitial volume to the total available interstitial volume, it can be written that:

$$A_{\text{BLOCKED}} = A_S \frac{V_{F,I}}{V_I} \quad (1)$$

where  $A_{\text{BLOCKED}}$  is the blocked screen area,  $A_S$  is the screen surface area,  $V_I$  is the total available interstitial volume and  $V_{F,I}$  is the volume of fibrous debris causing the blockage.

With this assumption, the screen area that remains open,  $A_{\text{OPEN}}$ , is found to be:

$$A_{\text{OPEN}} = A_S \frac{V_I - V_F}{V_I - A_S \Delta_F} \quad (2)$$

In the above equation,  $V_F$  is the total volume of fibrous debris in the sump and  $\Delta_F$  is the thickness of the “thin bed” of fibrous debris formed on the open screen surface area.

The volume of fibrous debris deposited as “thin bed”,  $V_{F,S}$  is determined as:

$$V_{F,S} = \left( A_S \frac{V_I - V_F}{V_I - A_S \Delta_F} \right) \Delta_F \quad (3)$$

**II. BASE CASE SCENARIO CALCULATION**

Using the data for the base case scenario calculation, the participating quantities are:

$$A_S = 1,139 \text{ ft}^2 \text{ (Reference [6], page. 1)}$$

$$V_F = 125.9 \text{ ft}^3 \text{ (Reference [6], page. A-2)}$$

$$V_I = 157.77 \text{ ft}^3, \text{ (Reference [6], page. 14)}$$

It is noted that the interstitial volume equals the total volume of debris that can be modeled with a flat-plate type correlation such as NUREG/CR-6224 (Reference [6], page 14).

Assuming a “thin bed” thickness of  $\Delta_F = 0.125$  in, the open screen flow area is calculated as:

$$A_{\text{OPEN}} = 1,139 \text{ ft}^2 \frac{157.77 \text{ ft}^3 - 125.9 \text{ ft}^3}{157.77 \text{ ft}^3 - 1,139 \text{ ft}^2 \times 0.125 \text{ in} / 12} = 248.79 \text{ ft}^2$$

The volume of fiber deposited as “thin bed” is calculated as:

$$V_{F,S} = 248.79 \text{ ft}^2 \times 0.125 \text{ in} / 12 = 2.59157 \text{ ft}^3$$

The head loss for the base case scenario with uniform debris distribution was calculated assuming a screen surface area reduction of 47 ft<sup>2</sup> (Reference [6], page. 2). The head loss was found to be:

$$\Delta H_{\text{UNIFORM}} = 0.305 \text{ ft-water.}$$

This value is very close to the value reported for the base case scenario (Reference [6], page. A-3):

$$\Delta H_{\text{BASE CASE}} = 0.30 \text{ ft-water.}$$

The head loss for the base case scenario assuming a partial blockage of the interstitial volume and formation of a “thin bed” was calculated and the results are displayed in Figure I-2. The head loss was found to be:

$$\Delta H_{\text{BLOCKAGE}} = 0.164 \text{ ft-water.}$$

It is mentioned that the values for the specific surface areas were assumed to be equal to those used in the base case scenario calculation and reported in (Reference [6], page. 3).

### **III. BASE CASE SCENARIO CALCULATION WITH 15% INCREASE IN FIBER VOLUME**

For this sensitivity calculation, the fibrous volume was increased by 15% while keeping the remaining input data unchanged:

$$V_F = 1.15 \times 125.9 \text{ ft}^3 = 144.785 \text{ ft}^3.$$

Assuming a “thin bed” thickness of  $\Delta_F = 0.125$  in, the open screen flow area is calculated for this case as:

$$A_{\text{OPEN}} = 1,139 \text{ ft}^2 \frac{157.77 \text{ ft}^3 - 144.785 \text{ ft}^3}{157.77 \text{ ft}^3 - 1,139 \text{ ft}^2 \times 0.125 \text{ in} / 12} = 101.366 \text{ ft}^2$$

The volume of fiber deposited as “thin bed” is calculated as:

$$V_{F,S} = 101.366 \text{ ft}^2 \times 0.125 \text{ in} / 12 = 1.0559 \text{ ft}^3$$

The head loss for this case was first computed assuming uniform debris distribution and a screen surface area reduction of 47 ft<sup>2</sup> (Reference [6], page. 2). The head loss was found to be:

$$\Delta H_{\text{UNIFORM}} = 0.31734 \text{ ft-water.}$$

The head loss for this case assuming partial blockage of the interstitial volume and formation of a “thin bed” was next calculated and the head loss was found to be:

$$\Delta H_{\text{BLOCKAGE}} = 0.61278 \text{ ft-water.}$$

Thus, increasing the fibrous volume by 15% and assuming a partial blockage of the screen interstitial volume combined with formation of a 1/8 in “thin bed” on the remaining screen surface area leads to a significant increase in the predicted head loss.

It is noted that the increase in fiber volume while keeping the particulate content unchanged reduced the particulate-to-fiber mass ratio from 0.52323 down to 0.45498.

**APPENDIX II.  
CONFIRMATORY HEAD LOSS CALCULATIONS**

**Verify CR3 Submittal Calculations**

Two head loss calculations from CR3 Calculation M04-0007 were verified by reproducing the result using the NRC developed solver for the NUREG/CR-6224 Correlation (referred to as NRC-6224). Then the input problems were modified to match the NRC position on the GR and SE Guidance. The CR3 calculations simulated included: (1) base case calculation (CR3 M04-0007, Pages A-2 and A-3) and (2) thin-bed calculation (CR3 M04-0007 Pages A-60 and A-61). First an NRC-6224 calculation was done to reproduce each CR3 HLOSS calculation and then a second NRC-6224 calculation was done with input parameters determined by SE guidance and consistent with the CR3 calculational set. The calculation results are compared in Tables II-1 and II-2 for the base and thin-bed calculations, respectively.

**Table II-1. Base Case Calculation Comparison**

Parameter	CR3 HLOSS	NRC 6224 Correlation Verification of HLOSS	NRC 6224 Correlation Using SE Guidance
Head Loss (ft-water)	0.30	0.31	0.42
Approach Velocity (ft/s)	0.018	0.018	0.018
Uncompressed Bed Thickness (in)	1.384	1.384	1.60
Compaction Ratio	1	1	1
Bed Porosity	0.92	0.92	0.93
Particulate/Fiber Mass Ratio	0.52	0.52	0.52
Fiber Specific Surface Area (ft <sup>-1</sup> )	129,450	129,450	168,540
Particulate Specific Surface Area (ft <sup>-1</sup> )	144,760	144,760	161,320

**Table 2. Thin-Bed Case Calculation Comparison**

Parameter	CR3 HLOSS	NRC 6224 Correlation Verification of HLOSS	NRC 6224 Correlation Using SE Guidance
Head Loss (ft-water)	0.47	0.48	0.61
Approach Velocity (ft/s)	0.018	0.018	0.018
Uncompressed Bed Thickness (in)	0.385	0.385	0.385
Compaction Ratio	0.78	0.78	0.86
Bed Porosity	0.80	0.80	0.80
Particulate/Fiber Mass Ratio	1.7	1.7	1.9
Fiber Specific Surface Area (ft <sup>-1</sup> )	160,640	160,640	160,640
Particulate Specific Surface Area (ft <sup>-1</sup> )	153,080	153,080	168,520

A number of points can be made from these comparisons:

1. The CR3 calculations contain an inconsistent use of head loss parameters.
  - The mineral wool specific surface area in the base case was 129,450/ft compared to 160,640/ft for the thin-bed case (significant). The mineral wool glass density is 179-lbm/ft<sup>3</sup> in the base case and 176-lbm/ft<sup>3</sup> in the thin-bed case (minor).
  - The CR3 Table has 263 lbm of ZOI coatings debris but the thin-bed case uses 258 lbm. The base case uses 263 lbm (minor).
  - The CR3 Table has 94 lbm of unqualified coatings debris but the thin-bed calculation assumes 47 lbm (significant).
2. The GR conservatively recommends assuming 10 µm spheres for unqualified coating debris due to substantial uncertainty regarding knowing debris size, however CR3 M04-0007 treats unqualified coatings as chips where  $S_v=2/t$  and  $t=1\text{mil}$ . The specific surface area for 10 µm spheres is 182,900/ft compared to 24010/ft for chips (significant). An additional reason for assuming 10 µm spheres for unqualified coating debris is the development of the 6224 head loss correlation was based on particulates and may under represent the head loss associated with chip debris.
3. CR3 M04-0007 combines Nukon® and latent fibers with the mineral wool by calculating the volume of these two debris types in with mineral wool by assuming the 8 lbm/ft<sup>3</sup> bulk density for mineral wool applies to Nukon® and latent fibers, as well (i.e.,  $\text{volume}_{\text{Nukon}^\circledast} * 2.4/8$ ). This procedure is incorrect because each type of fibrous debris would essentially maintain its own volume within the bed. Therefore, the M04-0007 procedure incorrectly determines the bed thickness (note the SE base case thickness is 1.60-inch compared to 1.38-inch from M04-0007). The bed thickness error is not that substantial for CR3 because the fibrous debris is dominated by mineral wool, however in other situations the distribution could be more evenly split. The appropriate procedure according to NRC research and software is to maintain the correct volumes but then determine volume averaged properties for the mixture.
4. The HLOSS code apparently limits overall bed solidarity to a user input number, which in Reference [6] was set to 20%. The limiting solidarity affects the head loss for thin-bed debris beds. NRC-6224 implements an equation to limit compaction that is based on the constituent-specific properties for each constituent (fiber porosity and the sludge densities of each particulate) combined into an equivalent mixture. There is no specific reason why the solidarity must be 20%. While numbers are provided in the SE for the latent particulate, the solidarity for the coatings debris is not actually known. In the above NRC-6224 calculations, 20% solidarity was assumed for the coating debris. Nonetheless, 20% seems reasonable for coating debris postulated to be 10 µm spheres and likely provides reasonable head loss estimates for CR3. This HLOSS limitation might incorrectly calculate head loss for debris beds using other type of debris.
5. A compression function K value of one (see Reference [6] Page 6 of 37) was apparently applied to mineral wool ( $K=1$  is appropriate to Nukon®) but there is no specific reason why the value should be one for mineral wool. Reference [6] should justify  $K=1$  for mineral wool (e.g., there is so little compression predicted

at the low approach velocities that it does not matter). A value can possibly be determined from Alion mineral wool head loss testing.

6. The Reference [6] correctly reduced the effective screen area by 47 ft<sup>2</sup> to account for tag debris.

### Alternate Debris Accumulation Calculations

The CR3 strainer design has not been tested under quality assurance procedures, even as a scaled prototype, therefore debris accumulation patterns on the CR3 strainer are uncertain. The licensee's vendors did state that non-safety-related testing had been conducted but these tests were not reviewed by the audit team. Reference [6] apparently assumes the accumulation would occur non-uniformly but still involve essentially all screen surfaces. Due to the uncertainty in the debris accumulation patterns, three alternate debris accumulation patterns were evaluated to determine if any potential debris accumulation could cause significantly higher head losses than the Reference [6] estimates. These alternate accumulations include: (1) bottom packing in the top hat strainers, (2) circumferential accumulation, and (3) trash rack accumulation.

Bottom Packed Accumulation To develop this postulated bed formation the following is assumed:

1. All the debris entering the top hat strainer array settles or otherwise deposits towards the bottom of the units resulting in packed debris in the lower portion and free volume in the upwards portion.
2. Sufficient fiber deposits on the upper portion that a thin-bed of debris forms.
3. All water flows into the upper thin-bed portion of the strainer.
4. The percentage of the total particulate depositing onto the upper thin-bed portion formation is treated as a variable parameter.

The volumetric quantities of debris transported to the strainer includes: 15.6 ft<sup>3</sup> of Nukon® (Table 2-1), 117.5 ft<sup>3</sup> mineral wool (Table 2-1), 23 ft<sup>3</sup> of RMI (Page 22), and 12.5 ft<sup>3</sup> of latent fiber (30 lbm at 2.4 lbm/ft<sup>3</sup>) for an estimated total debris volume of 168.6 ft<sup>3</sup>. The total interstitial free volume for the strainer array is 252.5 ft<sup>3</sup>, therefore the lower 2/3 of the strainer is assumed to be debris packed (effectively blocking the flow) while the upper 1/3 is relatively free of debris. The area of the upper thin-bed portion is then 380 ft<sup>2</sup>.

The head loss was calculated assuming four different particulate loadings for the postulated thin-bed accumulation on the upper third of the strainers. These loadings were 6%, 10%, 20%, and 100% of the total particulate debris which includes 170 lbm of latent particulate, 263 lbm of ZOI qualified coatings, and 94 lbm of unqualified coatings. If the particulate was distributed uniformly with the fibrous debris, approximately 6% of the particulate would be deposited in the upper third of the strainers in this postulated accumulation scenario. The resultant head losses are shown in Table 3.

**Table II-3. Bottom Packed Accumulated Head Losses**

Particulate Deposited in Upper Third Thin-Bed	Head Loss (ft)
6%	0.28

10%	0.59
20%	1.0
100%	4.5

For particulate loadings in the upper third that are less than 20%, the thin-bed head losses are less than 1 ft of water. In order to create a high head loss, the particulate has to be concentrated in the upper one-third while the fiber is concentrated in the lower two-thirds of the strainer. Such a debris accumulation is not realistic. In conclusion, preferential fibrous debris accumulation at the lower portions of the strainer array will not cause excessive head losses.

Circumferential Accumulation Once a complex strainer becomes fully engulfed with accumulated debris, its effective strainer area approaches its circumscribed area. For the CR3 top hat design, the circumscribed area becomes the single vertical open face and the array top surface (the other three sides are sump pit walls). This total area is approximately 124 ft<sup>2</sup> [(7'7" + 4 x 14.5/12) x 10']. The audit team noted that with 50% more debris than currently predicted to transport to the sump screens, this strainer would be fully engulfed, whereby the circumscribed area would be applicable.

The gaps between the top hats in the array could block closed due to debris bridging the gaps without filling all of the array interstitial volume. From the side, the initial gap width is 2.35-inches, but with debris accumulation the width continues to decrease. The narrower the gap width, the more potential exists for bridging to occur. The top surface has entrance openings into the array that are initially 8-inches across, which would be much more difficult to bridge. Assuming a contiguous layer was to accumulate over the circumscribed area, the audit examined the potential head loss. The approach velocity to the circumscribed area is 0.16 ft/s; therefore debris compaction would be significant. A range of bed thicknesses and compositions would apply here but the following example illustrates the ease of blocking the circumscribed area should the spacing between the top hats bridge. Given 0.5-inch thick layer of mineral wool and a particulate to fiber mass ratio of 0.5, the predicted head loss is 2.5-ft. It would take about 5.2 ft<sup>3</sup> of the mineral wool or about 4% of the total mineral wool and about 4% of the available particulate to form this circumscribed layer. If bridging did occur, or the strainer array completely filled, the head loss could easily exceed the available NPSH margins. Note that M04-0007 does not address this issue.

Trash Rack M04-0007 assumes all debris approaching the trash rack passes through the rack to the top hat array screens. The analysis indicates that most large piece debris would not reach the trash rack. A reasonable assumption could be that a few large pieces would reach the trash rack but not enough to cover the trash rack flow area of approximately 100 ft<sup>2</sup>. On the other hand, some of the small debris would almost certainly hang up on the grating when the piece overlapped a bar. The licensee did not address how much debris caught by the grating it would take to form bridges across the 1.5-inch cells. This was not addressed in M04-0007 and no data is available for debris accumulation on a grating. As an example head loss prediction, assume a mineral wool layer that is 0.5-inches thick with a particulate to fiber mass ratio of 0.5; the predicted head loss across the trash rack is 3.2 ft. The approach velocity to the rack is 0.19 ft/s. If bridging did occur across the trash rack cells, the head loss could easily exceed the available NPSH margins. The audit team questioned a transport issue concerning whether or not large piece debris will saturate with water in a reasonable time to prevent floatation transportation to the sump. CR3 noted that their design includes large

openings in the trash racks to prevent blockage by large pieces of debris. The licensee should verify that if large pieces mineral wool float to the sump before sinking, blockage of the trash would remain unlikely.



## APPENDIX III.

### AUDIT REPORT OF HEAD LOSS TESTING SUPPORT CRYSTAL RIVER UNIT 3

#### 1.0 INTRODUCTION

Crystal River Unit 3 (CR3) sponsored head loss testing performed by Alion Science and Technology at the Alion test facility in their vertical head loss test loop located at 10 W 35<sup>th</sup> St. in Chicago, IL. The CR3 head loss calculations documented in CR3 calculation M04-0007, "CR3 RB Sump-Head Loss Calculation for Debris Laden Screen," used the NUREG/CR-6224 Correlation, as coded in the Alion HLOSS code, to estimate sump screen head losses. The purpose of the Alion head loss tests was: (1) to benchmark the NUREG/CR-6224 Correlation for application to CR3 debris, and (2) to determine an appropriate equivalent fiber diameter for mineral wool to specify its specific surface area for input into the correlation. Mineral wool is the predominant fibrous insulation at CR3.

CR3 provided the following documents for NRC review that pertain to the Alion head loss testing.

1. ALION-PLN-LAB-2352-02, Rev. 0, "Hydraulic Testing of Debris Program Description: Vertical Loop."
2. ALION-SPP-LAB-2352-21, Rev. 0, "Test Lab Safety Procedure."
3. ALION-SPP-LAB-2352-22, Rev. 0, "Debris Preparation Procedure."
4. ALION-SPP-LAB-2352-23, Rev. 0, "Hydraulic Testing of Debris Test Plan Guideline."
5. ALION-SPP-LAB-2352-31, Rev. 0, "Vertical Test Loop Fill Procedure."
6. ALION-SPP-LAB-2352-32, Rev. 0, "Vertical Test Loop Draining and Cleaning Procedure."
7. ALION-SPP-LAB-2352-33, Rev. 0, "Vertical Test Loop Debris Head Loss Procedure."
8. ALION-PLN-LAB-2352-51, Rev. 2, "Hydraulic Testing of Mineral Wool Debris Test Plan: Vertical Loop."
9. ALION-REP-LAB-2352-52, Rev. 0, "Hydraulic Properties of Mineral Wool Insulation Test Report."
10. ALION-PLN-LAB-2352-56, Draft, "Hydraulic Testing of NUKON<sup>®</sup> Debris Benchmark Test Plan: Vertical Loop."

On May 18, 2005, a team of NRC staff and its contractors visited the Alion test facility to examine the Alion Vertical Loop Test Facility and the associated test procedures used to obtain the CR3 head loss data. The audit team included the following NRC staff: David Solorio, Ralph Architzel, Shanlai Lu, Mark Kowal, Ralph Caruso, Brenda Mozafari, and consultants Clinton Shaffer of ARES Corporation, and Vesselin Palazov of ISL, Inc.

Principal representatives of Alion present during the visit included Gilbert Zigler and Robert Choromokos.

## **2.0 TEST APPARATUS**

The Alion head loss test loop was designed to measure the head loss across a debris bed formed on a screen in the vertical test section of the closed loop. The design of the Alion loop is similar to the Alden Research Laboratory (ARL) closed loop head loss test apparatus used to perform NRC sponsored head loss testing [NUREG/CR-6367] and the University of New Mexico (UNM) closed loop head loss test apparatus [LA-UR-04-1227].

The apparatus components include: (1) a vertical test section that houses a screen mounted on a support ring, (2) a 170-GPM capacity centrifugal pump drawing water from the bottom of the test section, (3) both small and large piping sections in parallel containing low-range and high-range flow transmitters, respectively, (4) a main butterfly control valve, (5) globe isolation valves, (6) a return line to the top of the vertical test section, and (7) a drain valve. Debris is introduced at the open top of the vertical test section. Instrumentation includes: (1) two differential pressure transmitters to record differential pressure across the debris bed, (2) small and large loop flow rate transmitters, and (3) two thermocouples to measure water temperature downstream of the test debris bed. Test data is feed into a computer where it is displayed and recorded on a time dependent basis using LabVIEW 7.1 data acquisition software.

Like the ARL and UNM test loops, the loop does not have capability to control temperature, i.e., neither a water heater nor a cooler. The test temperature was essentially the temperature of the water added to fill the test loop.

NRC Staff Audit The audit team examined the test apparatus and found the apparatus to be well designed and constructed. The following specific observations were made:

1. The support ring holding the test screen in place appeared to be firmly, squarely, and uniformly attached to the test section piping.
2. Any flow acceleration due to the orifice type of effect caused by the presence of the support ring should be nominal at the CR3 application test velocities.
3. The strainer screen was constructed from perforated plate comparable to the proposed screen for CR3.
4. Test specified flow rates were apparently easily maintained.
5. Neither water leakage nor mechanical vibrations of significance were observed.
6. Air accumulations below the test debris bed due to deaeration were noted, however at the test head losses observed, the air accumulations were minor and did not adversely affect head loss measurements.
7. Water temperature increases due to pump heating were relatively small due to the relatively low test pump flow rates.

The audit team recommended that Alion implement the ability to monitor water turbidity as a relative measure of the filtration efficiency of the debris bed tested. For the CR3 particulate tested, this is a relatively minor concern, however in debris testing of very fine particulates (e.g., calcium silicate), turbidity measurements are necessary to evaluate the amount of calcium silicate debris residing in the debris bed.

## **3.0 TEST PROCEDURES**

Alion test procedures were provided in the documents listed above. The audit team reviewed the procedures and observed the implementation of some of the procedures during the team's visit to the Alion facility.

### **3.1 Vertical Test Loop Fill Procedure**

The initial step in conducting a head loss test is filling the test loop with water. A detailed procedure for filling the test loop was provided in ALION-SPP-LAB-2352-31, Rev. 0, "Vertical Test Loop Fill Procedure." This procedure prescribed the proper opening and closing of valves that close the test loop drains, initiate water flow, terminate water flow when filled, and establish the proper valve positions for the test. When the test calls for hot water, the hot water faucet valve is opened for a supply of hot water.

NRC Staff Audit The test loop was already filled when the audit team arrived to observe testing but the team examined the water fill procedure and found the procedure to be thorough and adequate for successful testing. However, the team noted that the water temperature introduced into the test loop is not controlled, i.e., the temperature of the hot water is whatever is available at the faucet. The temperature of the available hot water was not noted in the procedure documents.

### **3.2 Debris Preparation Procedure**

The debris preparation procedure is one of the most important aspects of successful head loss testing. Alion provided a procedure describing the preparation of fibrous debris and calcium silicate in ALION-SPP-LAB-2352-22, Rev. 0, "Debris Preparation Procedure." CR3 head loss estimates do not consider calcium silicate; therefore calcium silicate preparation is not discussed further here. A procedure was not provided for the inorganic zinc particulate. For fibrous insulation (e.g., NUKON® and mineral wool), the procedure prescribed first cutting the insulation into 12-inch squares, then processing the squares through a shredder. The shredded debris is compared to the size distribution classification system noted in NUREG/CR-6808, Table 3-2. Pieces of debris larger than Sizes 1 through 4 of this classification system are then to be further shredded by hand or discarded. If only a small amount of material is required, it is acceptable to shred the insulation by hand. For each specific test, the specified mass of fibrous debris is weighed out that meets the size distribution requirements. If the insulation is new (i.e., not aged), the shredded debris is boiled in water for 60 minutes, then placed in a bucket of water with a temperature that closely matches the test temperature water, and then further beat with a paint mixing stirrer for five minutes or until a homogeneous slurry is formed.

NRC Staff Audit The audit team was not present while fibrous insulation was being shredded but did observe NUKON® being boiled. The team made the following observation regarding debris preparation:

1. The procedure does not specifically discuss preparation of aged debris following the shredding process. The aged debris will also have to be introduced into water and become water saturated so it does not float in the test loop.
2. Small quantities of debris that was apparently floating in the top of the test loop were observed during the demonstration test to approach the test screen relatively late in the test. A likely reason for the floatation was that this debris still

- contained trapped air within the fibers. It is recommended that a step be added to the debris preparation procedure, that once the debris is boiled, the boiled debris should be kept underwater to prevent re-entrainment of air within the fibers.
3. Because a process such as hand shredding is not readily standardized, hand shredding should be kept to a minimum.
  4. The fibrous debris preparation approach used at UNM could be investigated as an alternate to ensure conservative head loss prediction. The UNM approach further processed the debris using a food blender to create finely shredded debris. This would more closely simulate debris beds formed by suspended individual fibers. A comparison between the UNM and Alion approaches would provide a useful gage for effects of debris fineness on head loss.
  5. The debris preparation procedure used in the laboratory to prepare inorganic zinc particulate debris for introduction into the test loop should be added to the written procedure.
  6. A debris preparation log should be maintained that identifies the source of the material, dates and times of preparation, and any deviations from the established procedure. For example, the properties of mineral wool depend upon the manufacturer and manufacturing process. Therefore, application of the test data is dependent upon assuring the mineral wool tested is the representative of the mineral wool in a specific plant.

Overall, the team found the debris preparation procedures to be adequate. However, the procedures could be improved by addressing the above considerations.

### **3.3 Vertical Test Loop Debris Head Loss Procedure**

The Alion procedure describing head loss testing was provided in ALION-SPP-LAB-2352-33, Rev. 0, "Vertical Test Loop Debris Head Loss Procedure." The purpose of this procedure is to identify the steps necessary to perform debris head loss testing in the vertical test loop. This procedure prescribes the operation of the vertical test loop during a head loss test including: (1) the establishment of initial valve placements, pump operation, and flow conditions, (2) the operational requirements for instrumentation and data acquisition system, (3) the introduction of debris into the test loop, (4) the operational variation of the test plan flow velocities, and (5) the termination of the test. Prerequisite requirements prior to initiating the head loss test procedure include: (1) filling the loop per the loop fill procedure, (2) ensuring the strainer has been properly installed in the test loop, (3) specified debris quantities have been prepared, and (4) a test plan containing a test matrix specifying the test conditions and acceptance criteria is available. An operational head loss pressure differential limit of 4 ft-water was declared. The procedure directs that the low flow path should not be used whenever the pump flow is greater than 50 GPM to protect the low flow meter.

NRC Staff Audit The NRC audit team made the following observations regarding its review of Alion test procedures, test plans, and the mineral wool test report.

1. The primary means of benchmarking the instrumentation was not readily apparent for each of the instruments.
  - a. For the differential pressure measures, the operational checklist called for ensuring all air was bled from the instrument tubes and that the correct clean screen head loss was indicated. There were two independent pressure transducers, but the procedures did not specify how closely

these instruments must agree before proceeding with the test. Missing from the documentation was the initial determination of the clean screen head loss for the type of screen present in the test. This determination would necessarily consider zeroing out the static head loss associated with the placement of the differential pressure taps in the test section.

- b. Three different thermocouples indicate the water temperature, backed up with an independent visually read temperature measurement, thereby ensuring quality temperature measurements. However, the required agreement among the measurements was not specified in the operational checklist.
2. The process of introducing debris into the test loop to form the debris bed is an important aspect of a successful test. When the purpose of the test is to determine appropriate properties for the NUREG/CR-6224 correlation, the test debris bed should be homogeneous and uniform. The head loss test procedure prescribes adding the debris slowly in accordance with the test matrix over a time period in excess of one minute and to observe the formation of the debris bed, which is expected to be homogeneous and uniform. The previous steps established the loop flow at 40 GPM corresponding to an approach velocity of approximately 0.1 ft/s. The team noted the following important considerations missing from the procedure:
    - a. Whether the zinc was premixed with the fibrous debris before introduction or were the components introduced separately. During the demonstration testing, the components were added separately leading to observed stratification.
    - b. The procedure does not include any criteria for determining whether or not the debris bed is homogeneous and uniform. Some reliable gage is needed to declare the test viable or not viable. For example, thickness measurements at different locations or perhaps a laser beam placed perpendicular to the test chamber wall might be used to quantify uniformity.

Alion technicians were observed to use a “fluffing” technique to stir up an existing debris bed to get the bed to reform. Neither a procedure nor success criteria was provided for this procedure. Upon examining the test logs included in the mineral wool test report, it is apparent that this procedure is used to transition from lower debris loadings to higher debris loadings within a specific test (e.g., the transition between Test 3 Q1 to Test 3 Q2 occurred in 15 min, therefore that bed must have been reformed). Apparently, the increase in debris is added to the loop, then the debris is ‘fluffed’ to homogenize and then allowed to settle back onto the screen. As such, the fluffing technique has the potential of altering the primary test result if the technique is not properly performed. The audit team noted that this technique has not been previously observed; therefore the success of this technique has not been previously established. The team’s concern is that with the fluffing technique, the debris is more bunched and closer to the screen when allowed to settle than when introduced slowly at the top. During the demonstration test, non-uniformities following fluffing were observed. The flow velocity at the time of fluffing is also important and should be incorporated into a fluffing procedure. The audit team considers that qualification testing of the fluffing technique, using approved procedures, should be performed to verify this technique creates debris beds that

provide conservative head loss results. Such testing should compare head loss test results of test conducted with and without fluffing.

The head loss test procedure incrementally increases or decreases the head loss in step changes allowing the head loss to stabilize at each step. This procedure is in accordance with head loss testing performed at other laboratories. The important consideration is that relative steady state is achieved at each step with regards to particulate filtration and head loss. The Alion procedure criterion for the steady state is that the change in head loss (increase or decrease) is less than 1% in a 10 minute period. In addition, sufficient time must have elapsed for water flow in the test loop to have completely circulated (referred to as a turnover) more than 5 times. The NRC audit team found the criteria acceptable for the CR3 debris tested but cautions that more time may be needed when a particulate like calcium silicate is tested.

3. According to the mineral wool test report, an experimental evaluation of the NUREG/CR-6224 compression function coefficients was a test objective, if possible. Yet, the test logs included in the mineral wool test report did not record any debris bed thicknesses. The audit team recommends that the Test Log form (Attachment A to ALION-SPP-LAB-2352-33, Rev. 0) be modified to include a column(s) for recording the debris bed thickness(s). In addition, the team recommends standardizing the measurement technique and including the technique in the head loss test procedure. Alion could consider fixing finely graduated scales at 2-4 locations around the test chamber so that eye-level measurements could be made reliably.
4. A procedural step needs to be added to the procedure that ensures all floating debris sinks onto the debris bed before test data is taken. An alternative would be to collect such debris, dry and weigh so that the correct debris bed mass can be deduced during analysis. Floating debris was observed in the demonstration test.
5. The NRC audit team noted that the test crew appeared to be well trained and conscientious in performing their duties.

### **3.4 Vertical Test Loop Draining and Cleaning Procedure**

The final step in conducting a head loss test is draining the water from the test loop and cleaning the loop prior to the next test. A detailed procedure for draining and cleaning the test loop was provided in ALION-SPP-LAB-2352-32, Rev. 0, "Vertical Test Loop Draining and Cleaning Procedure." This procedure ensured the strainer was removed from the test loop, prescribed the proper opening and closing of valves to drain the loop, specified washing the vertical loop from the top to the test section using a hose, prescribed a fill and flush of the loop, and a final drain. The procedure was to be repeated as many times as required to completely clean the vertical loop of any debris.

NRC Staff Audit The audit team did not observe the drain and cleaning procedure but the team examined the draining and cleaning procedure and found the procedure to be thorough and adequate for successful testing with the following exception. The test procedures do not specify the removal of the test screen and debris bed from the test section for subsequent examination.

### 3.5 Procedure for Determination of Basic Densities

The CR3 head loss analysis using the NUREG/CR-6224 correlation requires input values for the material and bulk densities of each of the debris constituents. For mineral wool, a material density of 179-lbm/ft<sup>3</sup> was apparently adapted from a generic source and the bulk density of 8-lbm/ft<sup>3</sup> was determined by the debris bed height in the vertical test loop. For inorganic zinc, a material density of 437-lbm/ft<sup>3</sup> was also apparently adapted from a generic source and the bulk density not determined. During the NRC audit team visit to the Alion head loss test facility, a laboratory technician commented on attempts to measure these properties in that laboratory for the specific material tested.

NRC Staff Audit The audit team recommends debris specific determination for these debris properties whenever reasonably possible rather than adapting data from a generic source. Such experimental determinations reduce uncertainty associated with variations in manufacturing processes, even by one manufacturer. However, such determinations can introduce uncertainty if the tests are not properly conducted. The team makes the following specific comments on density determinations:

1. Well established laboratory techniques exist for determining the material densities (i.e., specific gravities) of solid materials. Water displacement may work well after accounting for vaporization and water density changes provided all air entrained within the debris is removed. Removal can be a real difficulty with a material like calcium silicate.
2. The bulk density of fibrous debris, as used in NUREG/CR-6224, has been its density as-manufactured. The process of shredding the mineral wool likely alters that density; therefore the bulk density measurement made inside the Alion test loop of 8-lbm/ft<sup>3</sup> may differ from the as-manufactured density. The bulk density calculated from the dimensions of a geometrically shaped piece of undamaged insulation and its weight would provide a better as-manufactured density. The argument of whether it is better to use the as-manufactured density or the debris bulk density once in the test loop is difficult to address but using a true as-manufactured density is consistent with previous use of the correlation. That said, as long as the input values to the correlation show consistent and reliable conservative head loss predictions, the input values are satisfactory for that application.
3. The bulk density of the inorganic zinc (also referred to as the sludge density) can be readily assessed by measuring bulk volumes of dry material and the mass of material in the volume. This density has a key effect on debris bed solidarity limit where inorganic zinc limits the bed compression, which was one of the stated test objectives.

### 4.0 MINERAL WOOL TEST PLAN AND TEST REPORT

The mineral wool head loss testing for CR3 is documented in: (1) ALION-PLN-LAB-2352-51, Rev. 2, "Hydraulic Testing of Mineral Wool Debris Test Plan: Vertical Loop," and (2) ALION-REP-LAB-2352-52, Rev. 0, "Hydraulic Properties of Mineral Wool Insulation Test Report." The test objective was to develop head loss test data for mineral wool insulation that can be used to determine the material parameters of solidarity and specific surface to volume ratio. The test program objectives included: (1)

the validation of the technical basis for the applicability of the NUREG/CR-6224 correlation to debris on sump screens, and (2) obtaining generic hydraulic characteristic data of insulating materials to support confirmatory evaluation of sump screen performance for PWR plants. Mineral wool was tested by Alion with and without the addition of inorganic zinc particulate. The Alion test matrix consisted of four tests numbered 1 through 4 but Tests 1 and 3 each had three parts. Effectively, eight total head loss tests were conducted. The nominal uncompressed bed thicknesses ranged from about 1.4 to 1.9-inches thick and the particulate to fiber mass ratios were either zero or about 0.17.

NRC Staff Audit The audit team made the following observations regarding the Alion mineral wool head loss tests:

1. None of the tests created a compression limited condition whereby the solidity limit could be deduced from the test data. Specifically, thin-bed conditions were not included in the test matrix. Therefore, the objective of determining the limiting solidarity was not achieved. Note that in the CR3 head loss thin-bed evaluation, a limiting solidarity of 20% was assumed.
2. It is clear from the test data that a hysteresis effect was not evident at the velocities tested. This determination is important because the debris was introduced at a velocity higher than the general range of test velocities.
3. The specific surface area of the inorganic zinc was not experimentally determined. The CR3 head loss evaluations assumed a particle diameter of 10  $\mu\text{m}$  to calculate the specific area (i.e.,  $6/\text{diameter}$ ). The 10  $\mu\text{m}$  minimum diameter was a manufacturer stated minimum, which appears to be conservative. Still, an SEM analysis of the particulate, as tested, would verify a minimum size.
4. The analysis of the report deviated from the test program objectives of deducing the specific surface area from the head loss data. Rather, the analysis presented used a specific surface area corresponding to 10  $\mu\text{m}$  diameter fibers (i.e.,  $4/\text{diameter}$ ) and then showed the analytical results to be significantly higher than the experimentally measured head losses, i.e., input values leading to conservative predictions. This result highlights the importance of the comments previously made above regarding debris bed formation. If a tighter, firmer debris bed was formed by introducing finer debris, would the experimental head losses come closer to the correlation predictions? Is the disagreement between the correlation predictions and the test data due to the correlation or to the test data? The audit team is concerned that debris beds formed during Alion testing (e.g., specifically using the fluffing technique) do not create head losses as high as would be created using finer and slower debris accumulations.
5. A test program objective was to determine generic hydraulic characteristic data of insulating materials to support confirmatory evaluation of sump screen performance for PWR plants. However, the manufacture of insulations like mineral wool can vary with manufacturer and possibly between productions at a specific manufacturer. Therefore, application of the mineral wool data obtained for CR3 should be shown to be applicable for another PWR evaluation. Also the licensee should document the source of the mineral wool to confirm applicability to CR3.



## 5.0 NUKON® TEST PLAN

Alion provided a draft test plan for NUKON® insulation, i.e., ALION-PLN-LAB-2352-56, Draft, “Hydraulic Testing of NUKON® Debris Benchmark Test Plan: Vertical Loop.” The purpose of this plan is to obtain the hydraulic characteristics of NUKON® debris using the vertical test loop.

NRC Staff Audit The audit team reviewed this draft report. The team noted that the procedure would “Benchmark” the Alion NUKON® test data.

## 6.0 QUALITY ASSURANCE

The Alion program is implemented and maintained in accordance with the Alion Science and Technology Solutions Operation (ITSO) Quality Assurance Program for nuclear safety-related services. The Alion ITSO Quality Assurance Program states that it meets the quality requirements of 10CFR50, Appendix B, and ASME NQA-1-1989 for commercial nuclear power plants.

NRC Staff Audit The audit team noted Alion statements regarding their quality assurance program but did not review the Alion ITSO Quality Assurance Program.

## 7.0 DEMONSTRATION TEST OBSERVATIONS

The audit team observed demonstration testing performed for the team. This section documents team observations made regarding those tests.

### 7.1 Description of Tests Observed at the Alion Vertical Head Loss Loop

The initial loop conditions and the experiments observed during the visit to the Alion Hydraulic Lab are described in the following sections.

#### 7.1.1 Initial Loop Conditions

At the beginning of the visit to the Alion Hydraulic Lab that houses the Vertical Loop Test Facility, the experimental rig was already preconditioned and in a steady-state mode of flow recirculation with the debris bed established. The initial characteristics of the debris bed and major loop conditions are given in Table 1 below.

TABLE 1: INITIAL CHARACTERISTICS OF THE DEBRIS BED AND MAJOR LOOP CONDITIONS

Parameter	Units	Value	Note
Fibrous Debris	--	NUKON®	
Particulate debris	--	Not present	
Mass of Fiber	Lbm	0.32	
Mass of Particulate	Lbm	0.00	
Fluid Velocity	ft/s	0.05	Corresponding flow rate of ~17.6 gpm

Bed Thickness	In	~1 ¼	Uncompressed bed
---------------	----	------	------------------

### 7.1.2 Description of Experiments Observed

Two groups of experiments were performed during the visit at the Alion Vertical Loop Test Facility:

- (1) Experiments with a debris bed containing only fiber (NUKON®) and
- (2) Experiments with a debris bed composed of NUKON® fibers and inorganic zinc (IOZ) particulates.

These two groups of experiments are described separately in the following sections.

#### 7.1.2.1 Experiments with a Debris Bed Containing Only Fiber

Alion head loss predictions for NUKON®™, documented in ALION-PLN-LAB-2352-56, were performed using HLOSS by assuming a specific surface area of 171,673.83/ft, which corresponds to an accepted diameter for NUKON®™ fibers of 7.1 µm.

With the preconditioned fibrous fiber bed in place, the pump flow rate was increased stepwise by opening the butterfly valve located downstream from the pump exit. After each change of flow rate, steady-state loop conditions were achieved before obtaining a record for the head loss across the debris bed. Table 2 lists the test matrix and the observed (preliminary) head losses.

**TABLE 2: OBSERVED TESTS FOR A FIBROUS BED WITH NO PARTICULATES**

Test No.	Mass of Fiber (lbm)	Mass of Particulate (lbm)	Particulate-to-Fiber Mass Ratio (-)	Approach Velocity (ft/s)	Head Loss (ft-water)
Test 1	0.32	0.0	0.0	0.05	0.38
Test 2	0.32	0.0	0.0	0.10	0.85
Test 3	0.32	0.0	0.0	0.15	1.6

#### 7.1.2.2 Experiments with a Debris Bed Containing Both Fiber and Particulate

After the completion of the first test series, 0.036 lbm of IOZ were added while keeping the fibrous content of the bed unchanged (0.32 lbm of NUKON®). The particulate powder consisted of IOZ particles ranging in diameter from 10 to 100 µm. Alion conservatively assumed the inorganic zinc to be uniform spheres with a diameter of 10 µm with a corresponding specific surface area of 182,880/ft.

The fibrous and particulate ingredients were mixed applying a water jet in order to homogenize the bed content. Upon the sedimentation of the debris ingredients on the screen surface, the thickness of the formed uncompressed bed was measured to be approximately 1-¼ in. After stabilizing the loop flow at a rate that corresponded to a velocity of about 0.1 ft/s, a series of nine tests were performed. For Test 1, the head

loss for a homogeneous bed involving 0.32 lbm NUKON<sup>®</sup> and 0.036 lbm IOZ was measured. For the remaining six tests (Tests 2 through 7), certain predefined amounts IOZ were added incrementally to the loop flow so that a thin particulate layer involving an increasing content of IOZ was formed at the upper surface of the debris bed. During this process, the loop flow velocity was kept steady-state at 0.10 ft/s.

For Test 8, the pump was turned off and a water jet was used to mix the particulate layer, accumulated at the upper surface of the debris bed, with the fiber component. At a steady-state loop flow rate of 0.10 ft/s, the head loss was recorded. For Test 9, the pump was turned off and the debris bed was mixed once again applying a water jet. Then, the head loss was measured again at the same loop flow rate of 0.10 ft/s.

Table 3 lists the test conditions and the (preliminary) head losses observed for the experiments that involved both fiber and particulate.

**TABLE 3: OBSERVED TESTS FOR A DEBRIS BED INVOLVING FIBER AND PARTICULATE**

<b>Test No.</b>	<b>Fiber Mass (lbm)</b>	<b>Mass of Particulate Mixed with Fiber (lbm)</b>	<b>Mass of Particulate Added (lbm)</b>	<b>Head Loss at Approach Velocity of 0.10 ft/s (ft-water)</b>	<b>Note</b>
1	0.32	0.036	0.0	0.69	Homogeneous bed
2	0.32	0.036	0.036	0.69	Particulate layer
3	0.32	0.036	0.072	0.83	Particulate layer
4	0.32	0.036	0.072	1.0	Particulate layer
5	0.32	0.036	0.072	1.2	Particulate layer
6	0.32	0.036	0.072	1.4	Particulate layer
7	0.32	0.036	0.072	1.9	Particulate layer
8	0.32	0.432	0.0	1.0	Homogeneous bed
9	0.32	0.432	0.0	1.17	Homogeneous bed

## 7.2 Comments on the Test Methodology Applied

Several comments that consider the effects of major test parameters on head loss information collected with the test methodology applied are given in the following sections.

### 7.2.1 Approaching Fluid Velocity

As the experimentally obtained head loss data are related to the entire area of the debris bed, which is supposed to fully obstruct the cross-sectional area of the test section, ideal test flow conditions would involve a uniform (flat) radial velocity profile. Under such hypothetical flow conditions, the debris bed area is hydraulically loaded in a uniform manner. For a confined flow in a circular test section (pipe), the velocity profile most closely resembles a flat radial distribution when the flow is fully turbulent and the cross-

sectional plane of interest is located at a considerable distance downstream from the pipe inlet so that the flow pattern is fully developed. Under such flow conditions, the effects of the test section wall on the radial velocity profile near the debris bed location are confined within a narrow area adjacent to the channel wall. The thickness of this area corresponds to the thickness of the turbulent boundary layer.

Under a non-uniform approaching velocity distribution, the debris bed would be loaded non-uniformly with the bed areas that confront the maximum axial velocities experiencing the maximum pressure gradients and compression ratios. As a result, the obtained average head loss can differ from the head loss produced by a uniformly loaded debris bed when the approaching radial velocity profile is flat.

The Alion Vertical Loop Test Facility ranges of operation with respect to the approach velocity and fluid temperatures are as follows:

- (1) approach velocity range: 0.008 ft/s to 0.20 ft/s (0.0024 m/s to 0.061 m/s) and
- (2) fluid temperature: 60 °F to 110 °F (15.56 °C to 43.33 °C).

The fluid properties that correspond to the above temperature range are given in the table below. The values for the water density and dynamic viscosity listed in the table are computed using the industrial standard IAPWS-IF97.

**Table 4: Water Properties at the temperature range of operation of the Alion Vertical Loop**

Temperature, T		Density, $\rho_L$		Dynamic Viscosity, $\mu_L$	
(°F)	(°C)	(kg/m <sup>3</sup> )	(lbm/ft <sup>3</sup> )	(kg/s/m)	(lbm/s/ft)
60	15.56	999.0	62.37	1.121E-03	7.533E-04
70	21.11	998.0	62.30	9.749E-04	6.551E-04
80	26.67	996.6	62.22	8.573E-04	5.761E-04
90	32.22	995.0	62.11	7.610E-04	5.114E-04
100	37.78	993.1	61.99	6.812E-04	4.577E-04
110	43.33	990.9	61.86	6.141E-04	4.127E-04

Using the above documented water properties and the internal diameter of the vertical test pipe (D=1 ft or 0.3048 m), the flow Reynolds numbers at different fluid velocities are given in the following table. The values were computed using the formula:

**Table 5: Reynolds Numbers for the Alion Vertical Loop Test Facility**

Temperature, T (°F)	Average Approach Velocity			
	0.008 ft/s	0.1 ft/s	0.15 ft/s	0.2 ft/s
60	662	8,279	<b>12,419</b>	<b>16,559</b>
70	761	9,510	<b>14,265</b>	<b>19,020</b>
80	864	<b>10,800</b>	<b>16,200</b>	<b>21,600</b>
90	972	<b>12,146</b>	<b>18,219</b>	<b>24,292</b>

100	1,084	<b>13,544</b>	<b>20,316</b>	<b>27,088</b>
110	1,199	<b>14,991</b>	<b>22,486</b>	<b>29,982</b>

The above table suggests that the Reynolds numbers computed with the averaged approach velocity for the Alion Vertical Loop correspond to both the laminar and turbulent flow regimes.

In addition, the entrance length for laminar flow can extend to a maximum axial distance of:

$$\frac{z}{D} = \frac{Re}{20}$$

For turbulent flow, the entrance region can extend to a maximum axial distance of:

$$\frac{z}{D} = 25 \div 40$$

#### NRC Staff Audit

It is seen that a fully developed flow regime can not be established for the Alion Test Loop considering the length of the test section. Nevertheless, it is desirable to collect data under flow conditions that correspond to average Reynolds numbers typical for fully turbulent flow ( $Re > 10,000$ ). Such flow conditions are indicated by the Reynolds numbers given in bold in the above table. Typically, this would be the case when  $V_L > 0.1$  ft/s and  $T > 80$  °F. Both conditions were satisfied during the tests performed for verifying the hydraulic properties of mineral wool insulation (Report **ALION-REP-LAB-2352-52**).

#### **7.2.2 Spatial Debris Distribution on Screen Surface**

This section addresses the spatial distribution of the debris material on the screen surface assuming that the debris properties themselves are homogeneous. The key factor for forming a representative sample of a debris bed is the spatial distribution of the debris material over the screen surface. For a horizontally oriented flat screen, the gravity force acts as a stabilizing factor that helps keeping the debris material attached to the screen even under zero flow conditions so that the initial distribution (spreading) of the debris material over the screen is preserved. As a result, the homogeneity in distributing the debris material over the screen surface during the initial process of bed formation is essential.

Usually, the debris material is introduced when the test section is already filled with water and in a recirculation mode of operation. When the debris material consists of fiber, it is important to implement a process of bed formation such that the bed thickness distribution is close to uniform over the entire screen surface area. A non-uniform distribution of the debris would produce a bed that involves localized areas of a thinner debris layer. Such areas act as flow bypass and reduce the measured head loss for a given total loop flow rate. For a uniform non-compressed bed, reducing by half the thickness of 50% of the debris bed area and spreading the excess debris material uniformly over the remaining half of the bed surface, would reduce the resulting head

loss by a factor of 1.33. The conditions considered for this example assume that the hydraulic bed resistance depends linearly on the local flow velocity (the laminar head loss term is predominant).

Another possibility for bypass formation is related to the near-wall region of the screen. If the debris material does not approach the wall surface, pockets of low resistance would exist in the near-wall region leading to effects similar to those described in the previous paragraph.

Inhomogeneity in the distribution of the debris bed thickness on the screen surface could explain the observed disparity in the head losses observed in Test 2 documented in Table 2 and Test 1 documented in Table 3.

### **7.2.3 Spatial Distribution of Particulate Content in Fiber Volume**

This section addresses possible effects associated with the presence of a particulate component in the fibrous debris bed. It is known that fine particles contribute to the blockage of porous areas present in a fibrous bed and increase significantly the surface-to-volume ratio of the resultant debris mixture.

If the particulate material has been imbedded homogeneously within the fiber volume at the beginning of the test, a fraction of the particulate content can be washed out from the bed and entrained with the liquid flow. As a result, this entrained fraction of the particulate will be transported to the upper side of the debris bed by the recirculating flow and eventually filtered from the fluid. A larger portion of the filtration will occur at the upper surface of the debris bed. This particulate transport mechanism can lead to the gradual displacement of particulate from the bulk of the debris volume and the formation of a layer enriched with particulate content at the upper surface of the bed. Such mechanism can lead to a gradual increase in the head loss associated with the inhomogeneity in the distribution of the particles in the fibrous volume.

### **7.2.4 Head Loss Extraction from DP Measurements and Error Analysis**

The head loss data are extracted from DP measurements. A DP reading integrates the effects of several components:

- (1) gravitational head determined by the difference in elevation of the DP taps,
- (2) wall friction pressure losses,
- (3) pressure loss caused by the clean strainer, and
- (4) head loss created by the debris bed itself.

Pressure losses associated with the last three factors contribute to a DP measurement if there is a flow recirculation through the loop. The difference between two DP measurements that involve a clean strainer and a strainer loaded with a debris bed respectively, would yield the debris bed head loss provided that the loop flow and fluid temperature were the same for both measurements.

A DP measurement that is produced under stagnant loop flow conditions would reflect only the gravitational head component, which can be computed knowing the water density (a function of the measured water temperature) and the elevations of the DP

measurement taps. DP readings under such conditions can be also used to calibrate the DP measurements and account properly for any drift observed in the DP readings.

An analytical error analysis can be performed to determine the error in the head loss measurements as a function of the partial errors associated with the measurements of the individual contributing parameters such as fluid temperature, flow rate/velocity, debris bed thickness, and tap elevations.

## **8.0 NRC AUDIT TEAM CONCLUSIONS**

The NRC audit team visited the Alion head loss test facility where the team examined the test apparatus and found the apparatus to be well designed and constructed. The audit team noted that the test crew appeared to be well trained and conscientious in performing their duties. CR3 provided documents for NRC review that provided Alion head loss testing procedures.

The SER describes the following the success criterion for obtaining test data used to determine applicable NUREG/CR-6224 correlation input parameters:

1. The test debris bed consists of some mixture of fibrous debris with or without particulate debris.
2. The debris bed should be relatively uniform.
3. The debris bed should be relatively homogenous.
4. The approach velocity should be perpendicular to the flow.
5. The debris accumulation, flow rate through the debris bed, the temperature, and the measured pressure differential across the bed should be relatively steady.
6. The quantities of debris in the bed should be known.

The Alion head loss test apparatus has the ability to meet all of these criteria but one test procedural area still needs further experimental verification regarding the quality of debris bed uniformity and homogeneity. Of specific concern is an undocumented procedure called “fluffing” to stir up an existing debris bed to get the bed to reform. Apparently, one use of this procedure is the addition of more debris to a previous test where the additional debris is added, then the debris is fluffed to make it homogeneous before letting the debris settle back onto the screen. This technique has not been previously observed in other head loss test programs. When the audit team observed the fluffing, it appeared that the debris was more bunched and closer to the screen before letting it settle than when introduced slowly at the top. Qualification testing or other evaluation technique should be considered to verify that debris bed formed using the Alion test procedures cause representative head losses. Some criteria are needed to gage whether or not the Alion debris beds formed beds leading to conservative head loss predictions. For example, a successful debris bed forming technique was used in the UNM testing, which formed uniform and homogenized debris beds. Such a technique could be used as a gage whether or not the Alion debris preparation and bed forming procedures formed conservative debris beds. In the mineral wool test report, the NUREG/CR-6224 correlation predicted significantly higher head losses than the experimentally measured head losses. The audit team’s concern is that the experimental head losses may be less because the debris bed does not have complete homogeneity due to residual spacing between the debris pieces that effective form flow channels interior to the bed. The proposed qualification testing would dispel this

concern if alternate bed formation techniques do not result in higher head losses than the current Alion technique.

The facility audit was not able to review testing of the top hat strainer designed for CR3 and the test matrix of the test data provided is sparse. Specifically thin-bed testing was not performed, only one particulate to fiber mass ratio was tested, and fiber beds thicknesses were limited to a range of about 1.4 to 1.9-inches thick.



## **APPENDIX IV. CRYSTAL RIVER TOP HAT STRAINER AIR TRAPPING PHENOMENON EVALUATION**

### **1. Background**

The purpose of this evaluation is to make use of Computational Fluid Dynamics (CFD) methods to assess the potential air trapping inside the Crystal River top-hat strainer array and its possible impact on the ECCS safety injection pumps performance during the long term cooling phase of a postulated LOCA. The recirculation water that is collected in the containment sump contains air in solution with a concentration that depends on the water temperature and is directly proportional to the partial pressure of the air. During the recirculation period, if the partial pressure of the air decreases, then part of the air in solution can be released in the form of gas bubbles (containing air and water vapor). This situation may occur if the flow experiences a pressure drop across the strainer screens where various types of debris, carried along with the recirculation water, can accumulate and form a flow resistance.

The source term for the air bubble generation can be derived analytically based on Henry's law applied to air-water solutions [80]. The purpose of this CFD analysis is to give an indication on the fate of gas bubbles following their release from the recirculating water. If the generated gas phase is dragged to the suction nozzle, a failure of the safety injection pump may result due to flow cavitation.

### **2. Analysis Approach**

#### **2.1 Geometry and Assumed Operating Conditions**

The geometry and operating conditions are taken from the new sump strainer design of Progress Energy's Crystal River 3 (CR3) nuclear power plant, developed in response to the US NRC issuance of the GSI-191 [6].

The geometry of a single sump strainer is illustrated in Figure IV- 1. A schematic of the strainer configuration is drawn in Figure IV- 2 (the design includes an array of 8 by 4 vertical strainers). During the recirculation phase of a LOCA, the CR3 sump strainers are fully submerged. The water enters the inner cylindrical portion of the strainer and is then redirected radially to the annulus region through the inner perforated grid. In parallel, the water also flows between the vertical strainers and enters the annulus through the external perforated grid. From the annulus, the water is discharged to the lower plenum of the sump from where it eventually reaches the pumps through the suction nozzle. The annulus is sealed at the top and the inner and outer fluid regions of the strainer are sealed at the bottom, so that the only available path for the flood water to reach the suction nozzle is through the perforated grids.

The assumed flow conditions are as follows [6]:

Isothermal Flow at  $T = 120 \text{ F} = 322 \text{ K}$ ;  
 Containment pressure  $P_0 = 14.5 \text{ psia} = 1 \text{ atm}$ ;  
 Volumetric Flow Rate (total for all strainers):  $8508 \text{ gpm} = 0.54 \text{ m}^3/\text{s}$ ;

## 2.2 Air Generation

Consider a point on the free surface of the water flood. For Henry's law, the equilibrium concentration of air in water at that point is:

$$C_0 = H(T_{w0}) * P_{\text{air},0} \quad (1)$$

where  $H(T_{w0})$  is the Henry's law constant at the temperature  $T_{w0}$  of the water at the free surface and  $P_{\text{air},0}$  is the partial pressure of the air at the free surface. The latter is a component of the total pressure of the containment atmosphere, given by

$$P_{\text{cont,tot}} = P_{\text{air},0} + P_{\text{vap},0} \quad (2)$$

The partial pressure of the water vapor,  $P_{\text{vap},0}$ , can be expressed as the product between the relative humidity of the containment atmosphere,  $RH_{\text{cont}}$ , and the saturation pressure corresponding to the temperature of the containment atmosphere,  $T_0$ :

$$P_{\text{vap},0} = RH_{\text{cont}} * P_{\text{sat}}(T_0) \quad (3)$$

Using (1), (2) and (3), the equilibrium concentration of air in the water at the flood surface elevation is:

$$C_0 = H(T_{w0}) * [P_{\text{cont,tot}} - RH_{\text{cont}} * P_{\text{sat}}(T_0)] \quad (4)$$

Consider now a point downstream from the strainer screen, at an elevation  $z$  measured downward from the flood level. Following the same procedure as before, with similar meaning of the symbols, the equilibrium concentration of air in water at that point is given by Henry's law as:

$$C_1 = H(T_{w1}) * P_{\text{air},1} \quad (5)$$

and the partial pressure of air is a component of the total pressure at that point:

$$P_{1,\text{tot}} = P_{\text{air},1} + P_{\text{vap},1} \quad (6)$$

The total pressure  $P_{1,\text{tot}}$  at that elevation  $z$  includes contributes from the hydrostatic head,  $r_w * g * z$ , and the pressure loss across the strainer screen,  $DP_{\text{loss}}$ :

$$P_{1,\text{tot}} = P_{\text{cont,tot}} + r_w * g * z - DP_{\text{loss}} \quad (7)$$

If air is released from the solution of water and air, then the generated bubble may contain both air and water vapor. We can define a relative humidity for the gas bubble such

that (assuming that the generated bubble has the same temperature as the water at that point):

$$P_{\text{vap},1} = RH_{\text{bubble}} * P_{\text{sat}}(T_{w1}) \quad (8)$$

Combining (5), (6), (7) and (8) leads to the equilibrium concentration of air in water at elevation  $z$  downstream from the strainer screen:

$$C_1(z) = H(T_{w1}) * [P_{\text{cont,tot}} + r_w * g * z - DP_{\text{loss}} - RH_{\text{bubble}} * P_{\text{sat}}(T_{w1})] \quad (9)$$

Notice that (7) gives a limit for the pressure drop across the perforated grid, assuming that the total pressure at elevation  $z$  is to be greater than the saturation pressure at the corresponding temperature, in order to avoid bulk boiling. That is:

$$DP_{\text{loss}} < P_{\text{cont,tot}} + r_w * g * z - DP_{\text{loss}} - P_{\text{sat}}(T_{w1}) \quad (10)$$

Consider now the difference between the equilibrium concentration of air in water at the flood elevation,  $C_0$ , and the equilibrium concentration of air at a point at elevation  $z$  downstream from the strainer screen,  $C_1$ :

$$DC(z) = C_0 - C_1(z) \quad (11)$$

Assuming isothermal flow (i.e.  $T_{w0} = T_{w1} = T_w$ ), (11) becomes:

$$DC(z) = H(T_{w1}) * [DP_{\text{loss}} - r_w * g * z + RH_{\text{bubble}} * P_{\text{sat}}(T_w) - RH_{\text{cont}} * P_{\text{sat}}(T_0)] \quad (12)$$

If  $DC(z) > 0$ , then air must be released from the water at that elevation  $z$  to respect the upper limit of air that can be dissolved in solution according to Henry's law.

Thus, if  $DC(z)$  is positive, this quantity gives the mass of air that is released per unit volume of the water solution. The air is assumed to be released, in the form of small bubbles, at that location where the pressure drop occurs. For the case in consideration, the air would be released within the debris layers attached to the perforated grids. The air mass generation rate per unit volume of the debris bed can be obtained as follows:

$$\dot{m} = \frac{\Delta C \cdot Q_w}{V_{\text{debris}}} \quad (13)$$

where  $Q_w$  is the volumetric flow of water and  $V_{\text{debris}}$  is the volume of debris accumulated on the screens.

## 2.3 CFD Analysis

## Computational Domain

Assuming axial symmetry, a two-dimensional computational domain was created using the ANSYS Workbench<sup>(R)</sup> software. A schematic of the 2D model is shown in Figure IV-3. The unstructured computational grid includes about 150,000 elements. The geometry data was specified according to the information provided in reference [6]. A pressure boundary condition at the inlet specifies the containment pressure at the flood level elevation. At the outlet, the strainer flow rate is specified. Symmetry boundary conditions are specified on the remaining outer boundaries. Inner walls are specified internally to the domain to separate the different regions, according to the geometry specifications. Each perforated grid and the corresponding debris layer are lumped together and modeled as two porous regions. Within the porous media, a mass source of air is specified to model the air generation and a momentum sink is imposed to model the pressure drop.

## Physics Specifications

The physical properties of air and water are assumed constant for the given temperature of 322 K and containment pressure of 1 atmosphere.

Isothermal flow was assumed. The physical specifications of this CFD model are to capture and describe for this problem the fundamental forces that act on the air bubbles, i.e. the buoyancy force tending to push the air out of the domain from the top to the containment atmosphere, and the interfacial drag exerted by the water on the bubbles, tending to entrain the bubbles towards the pump suction nozzle.

The characteristic diameter of the generated bubbles is assumed equal to the Laplace term expressing the mechanical equilibrium for a bubble:

$$D_{bubble} = \sqrt{\frac{\sigma}{g \cdot \Delta\rho}} = 2.65mm$$

where  $\sigma$  is the surface tension coefficient,  $g$  is the acceleration of gravity and  $\Delta\rho$  is the density difference between the liquid and gas phases.

From preliminary calculations, it emerged that the bubble coalescence process was particularly important for this problem and thus it needed to be modeled. A logic was specified using the ANSYS CFX<sup>(R)</sup> mixture model to account for two levels of interactions between gas and liquid, for small and larger coalesced bubbles.

The Schiller-Neumann model for the interfacial drag coefficient was used for the small bubbles [81]. A constant interfacial drag equal to  $8/3$  was used for the large bubbles [81].

The air generation was modeled by imposing to the debris regions the volumetric mass source given by equation (13).

The pressure drop across the porous (debris) regions was imposed and modeled as a sink for the momentum equation by specifying an inertial loss coefficient. Although the maximum predicted pressure drop in reference [6] is less than 1 ft-water, the imposed pressure drop for this calculation was assumed to be higher and close to 7 ft-water, which is the designed height of strainer.

### Calculation Sequence

A steady-state calculation was preliminarily executed without air generation, to initialize the velocity field and the pressure distribution. Next a transient calculation was executed to observe the behavior of the air as it is released within the porous debris regions.

### Results

The results of the steady-state initialization are reported in Figure IV-4 through IV-7. The results of the transient calculation are reported in Figures IV-8 and IV-9.

The steady-state initialization, without air generation, reveals that the radial flow and pressure drop across the porous regions are fairly constant along the vertical elevation. Thus, the air generation will be fairly uniformly distributed within the porous regions. As expected, as water flows radially from the inner and outer regions to the annulus, the water velocity profiles decrease in the external regions and increase in the annulus, with maximum velocity at the discharge to the lower plenum.

The transient calculation shows that essentially all the generated air is initially dragged into the annulus. After entering the annulus, part of the bubbles, at higher elevations, are transported upwards by buoyancy, which prevails on the low drag force exerted by the water flowing at low velocity in that region. These bubbles coalesce on the lower face of the annulus top plate, where the amount of air keeps accumulating with time. The remainder of the bubbles, entering the annulus at lower elevations, are transported downwards by the water flowing at higher velocity, and dragged into the lower plenum. As the water velocity abruptly decreases in the lower plenum, the entrained bubbles are transported by buoyancy and by the recirculating motion of water to the lower face of the strainer lower support plate, where they coalesce and keep accumulating with time.

These CFD simulations proved to be extremely difficult to set up and execute, due to the requirements of the problem. In particular, very different time scales exist: the faster time scale, on the order of a few seconds, is due to the flow of water; an intermediate time scale, on the order of a minute, is due to the slower migration of bubbles against the water flow; the slowest time scale, on the order of several minutes, is due to the slow

bubble generation process. The fastest time scale poses an upper limit to the time step size for the transient calculation, which required many hours of CPU time to simulate a few minutes of problem time. Also, the transient calculation proved to be very unstable as a substantial amount of air was accumulating in the computational domain, leading to unexpected code failures due to non-convergence. Therefore, the results reported in this document should be considered very preliminary and introductory to the development of a more stable and reliable model.

## **Conclusions**

From the preliminary evaluation, if air generation occurs within the debris layers, then the possibility of air entrainment downstream the strainer screens cannot be ruled out. The calculations from this initial model show that the air has the potential for accumulating and forming coalesced bubbles in the sump region, with little chance of being released by buoyancy to the containment. It is not clear at this point whether the air will be entrained into the pump as a stream of small bubbles or large slugs. Based on this preliminary evaluation, the NRC staff considers that the licensee should address this issue and consider whether large air slugs would either not form, or not be transported to the pump intake, or could otherwise be mitigated. During a review for proprietary information, Enercon (the licensee's vendor) noted that the CFD model that evaluated the potential for air trapping in the top hat modules did not take credit for the two vent holes at the top of the strainer modules providing a vent path. This statement was not further evaluated by the NRC staff.

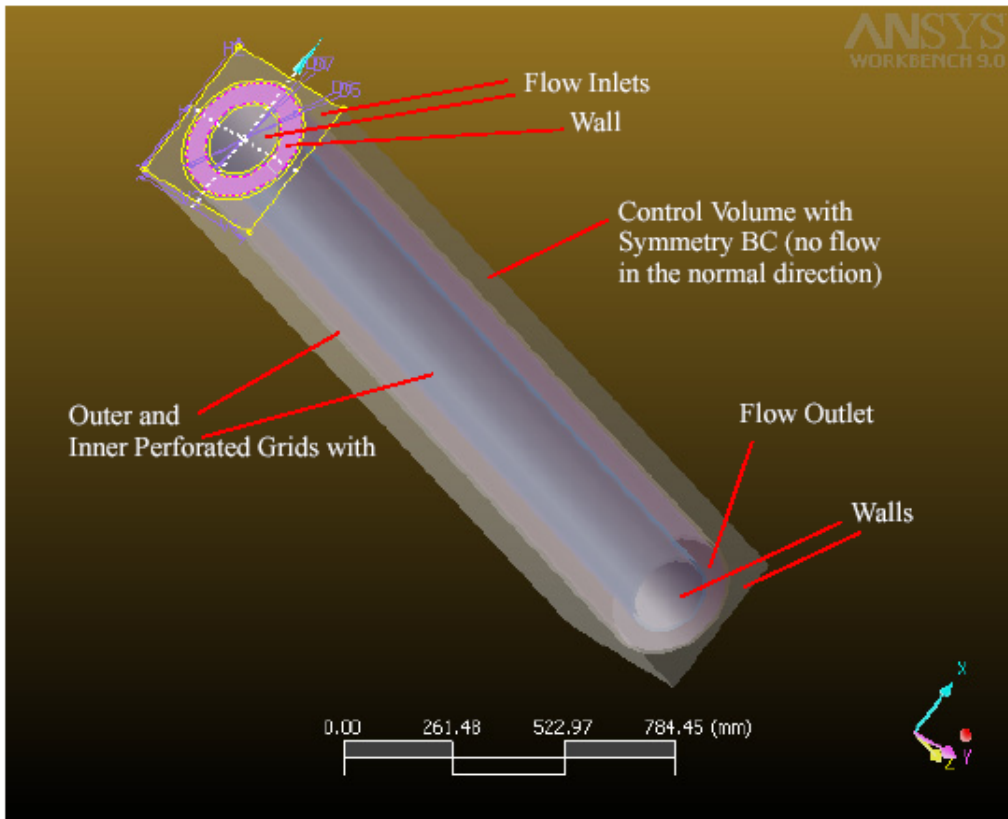


**Figure 1. Geometry**

Figure IV-1 Geometry.

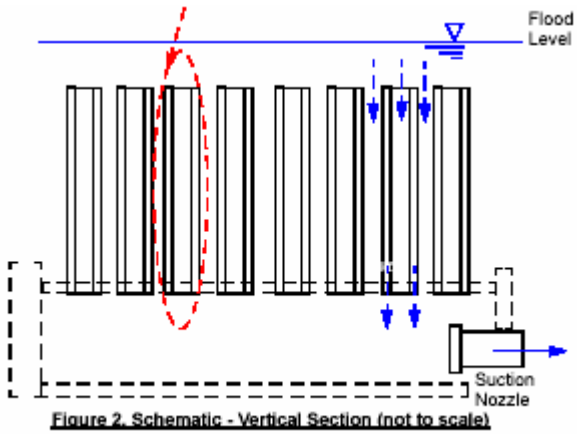
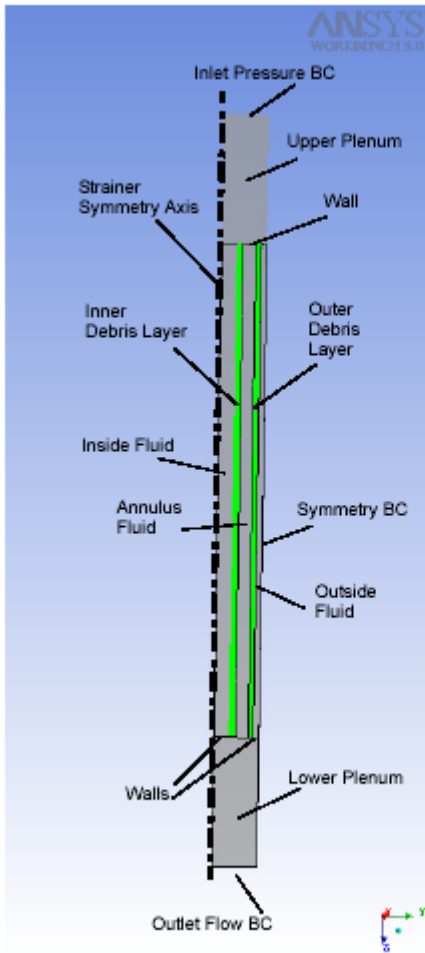


Figure IV-2. Schematic –Vertical Section (not to scale)





**Figure 3. Schematic of the 2D Computational Domain**

Figure IV-3 2-D Computational Domain.

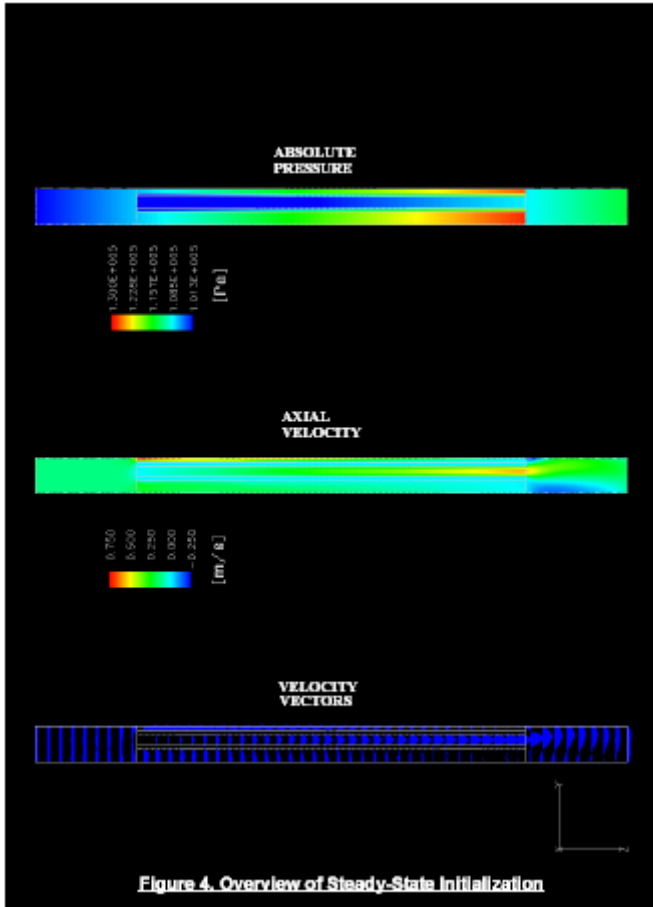
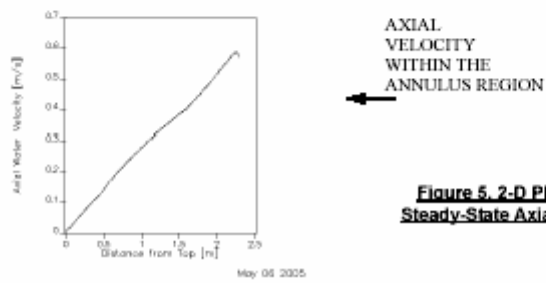
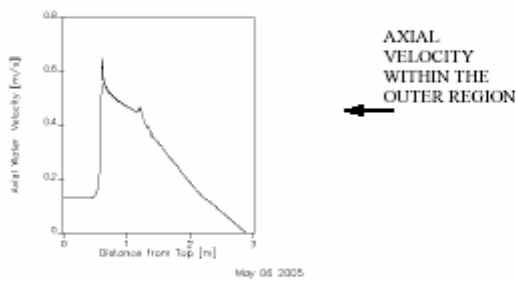
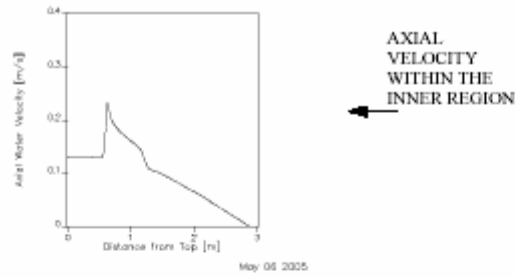
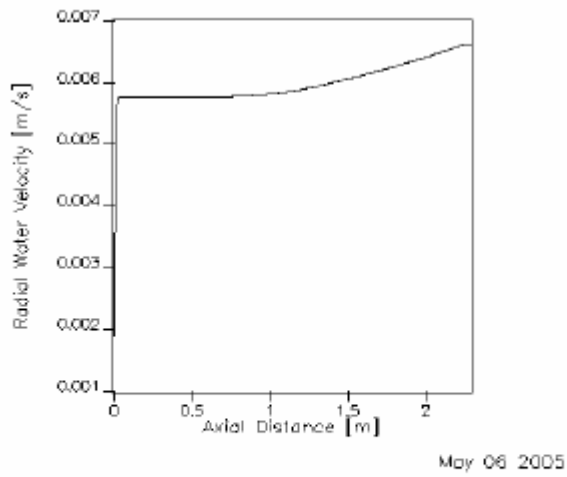


Figure IV-4 Overview of steady state initialization.



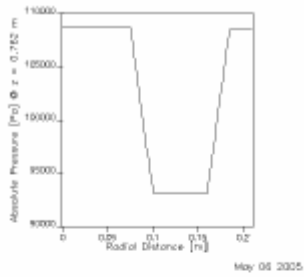
**Figure 5. 2-D Plots of the Steady-State Axial Velocities**

Figure IV-5 Plots of the steady state axial velocities.

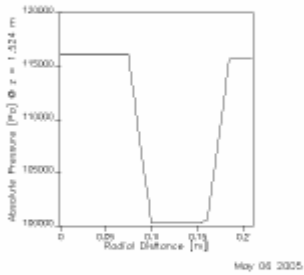


**Figure 6. Steady-State Radial Velocity of Water along the Inner Debris Layer entering the Annulus.**

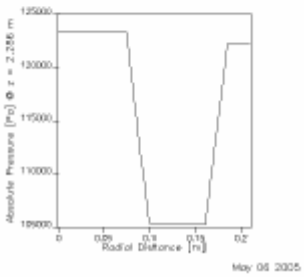
Figure IV-6. Steady State Radial Velocity of Water along the Inner Debris Layer Entering the Annulus.



AXIAL  
PRESSURE  
AT HIGHEST ELEVATION



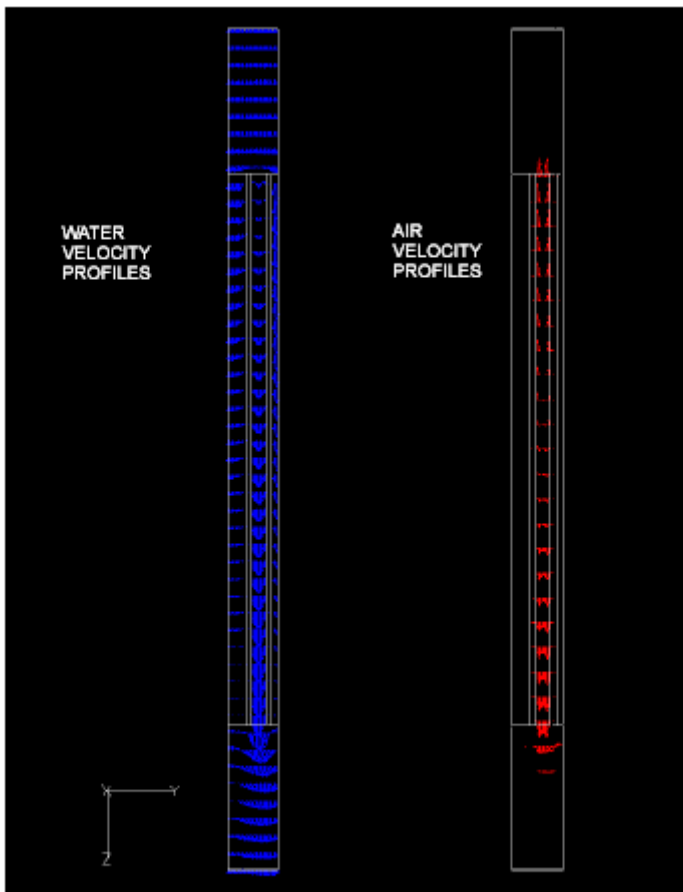
AXIAL  
PRESSURE  
AT INTERMEDIATE ELEVATION



AXIAL  
PRESSURE  
AT LOWEST ELEVATION

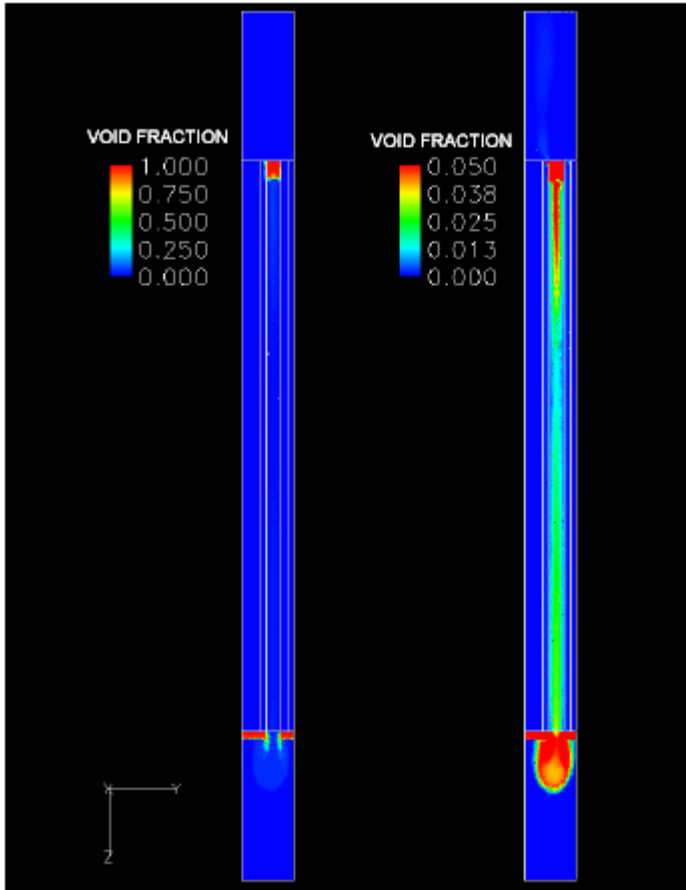
**Figure 7. 2-D Plots of the Steady-State Radial Pressure Profiles at different elevations**

Figure IV-7 2-D Plots of the steady state radial pressure profiles at different elevations.



**Figure 8. Water And Air Velocity Profiles at 3 min of Problem Time**

Figure IV-8 Water and Air Velocity Profiles at 3 min of Problem Time.



**Figure 9. Air Volume Fraction Distributions at 13 min of Problem Time (using two scales for the same void distribution)**

Figure IV-9 Air Volume Fraction Distributions at 13 min of Problem Time.